Polymer Chemistry

RSC Publishing

PAPER

View Article Online
View Journal | View Issue

Cite this: *Polym. Chem.*, 2013, **4**, 969

Thermally cross-linkable hole transporting polymer synthesized by living anionic polymerization for effective electron blocking and reduction of exciton quenching in multilayer polymer light emitting diodes†

Beom-Goo Kang,[ab] Hongkyu Kang,[ab] Nam-Goo Kang,[ab] Chang-Lyoul Lee,*[c] Kwanghee Lee[ab] and Jae-Suk Lee*[ab]

Received 6th September 2012
Accepted 15th October 2012

DOI: 10.1039/c2py20721d

www.rsc.org/polymers

A new cross-linkable polymer (d-P**BAB**), which has triphenylamine as the hole transporting moiety and ethynyl group as the thermal cross-linker, was synthesized by a living anionic polymerization and deprotection process. The thermally cross-linked d-P**BAB** layer had a smooth surface and excellent solvent resistance. The PLED fabricated with cross-linked d-P**BAB** as hole transporting layer (HTL) showed approximately one and half times higher luminance and four times higher luminous efficiency than those obtained from PLED with PEDOT:PSS. This is ascribed to better abilities of cross-linked d-P**BAB** to block electrons and prevent exciton quenching than those of PEDOT:PSS at the emitting layer (EML) interface. These results strongly suggested that cross-linked d-P**BAB** can be a promising material to replace conventional PEDOT:PSS.

Introduction

Polymer light emitting diodes (PLEDs) have been intensively studied as next generation flat panel displays due to their advantages such as easy and low cost solution processing, high brightness, fast response, and flexibility.[1–4] During the last two decades, the efficiency and lifetime of PLEDs have been dramatically improved as a result of extensive research efforts.

The efficiency of PLEDs strongly depends on the charge balancing, charge blocking, and exciton quenching processes. These requirements can be accomplished by multilayer device structure consisting of several functional layers such as hole injection and transporting layers (HILs and HTLs), electron blocking layers (EBLs), emitting layers (EMLs), and hole blocking and electron transporting layers (HBLs and ETLs).[5] In particular, to realize highly efficient PLEDs, the development of suitable HTLs is strongly required to maximize the hole injection and electron blocking and thus to confine excitons within the EMLs.[6] In addition, preventing exciton quenching at the interface of EMLs and near the electrode is another important role of HTLs towards enhanced device efficiency.[7]

Compared with small molecule based organic light emitting diodes (OLEDs) fabricated by vacuum deposition, the construction of multilayer structured PLEDs is more difficult because previously prepared layer can be harmed or dissolved by the organic solvent used for spin-coating the subsequent layer.[8] Therefore, water soluble poly(3,4-ethylenedioxythiophene):poly(styrenesulfonate) (PEDOT:PSS) has been widely used for the HIL and HTL in PLEDs due to its ease of processing without solubility issues as well as its high conductivity.[7,9,10] Despite these advantages, this conducting polymer has many drawbacks such as weak interface adhesion, inefficient hole injection, poor electron blocking abilities, and exciton quenching at the interface of the EML.[7,11–14] Furthermore, the acidity of PEDOT:PSS causes corrosion of the indium tin oxide (ITO) surface, which raises serious questions concerning the long term stability of devices.[15,16]

These drawbacks of PEDOT:PSS that lead to low device performance in PLEDs have been compensated for by inserting interlayers between the PEDOT:PSS and the EML.[5,7,17] Morgado *et al.* reported an almost two times improvement of the device efficiency in a fluorene based PLED by inserting poly(*p*-phenylenevinylene) (PPV) between the PEDOT:PSS and EML.[17] This enhancement of device efficiency originated from an improved charge balance within the EML due to the electron blocking effect of the PPV interlayer. Kim *et al.* reported a significant

[a]*School of Materials Science and Engineering, Department of Nanobio Materials and Electronics, Gwangju Institute of Science and Technology (GIST), 123 Cheomdan-gwagiro (Oryong-dong), Buk-gu, Gwangju 500-712, Korea. E-mail: jslee@gist.ac.kr*

[b]*Research Institute for Solar and Sustainable Energies (RISE), Gwangju Institute of Science and Technology (GIST), 123 Cheomdan-gwagiro (Oryong-dong), Buk-gu, Gwangju 500-712, Korea*

[c]*Advanced Photonics Research Institute (APRI), Gwangju Institute of Science and Technology (GIST), 123 Cheomdan-gwagiro (Oryong-dong), Buk-gu, Gwangju 500-712, Korea. E-mail: vsepr@gist.ac.kr*

† Electronic supplementary information (ESI) available: TGA of d-P**BAB**, TCSPC of d-P**BAB** and cross-linked d-P**BAB**, and CV of cross-linked d-P**BAB**. See DOI: 10.1039/c2py20721d

improvement of device efficiency in PLEDs with an added thin semiconducting polymer interlayer (~10 nm) between the PEDOT:PSS and EML.[7] The poly(2,7-(9,9-di-*n*-octylfluorene)-*alt*-(1,4-phenylene-((4-*sec*-butylphenyl)imino)-1,4-phenylene) (TFB) interlayer prevented the quenching of radiative excitons at the PEDOT:PSS interface by acting as an efficient exciton blocking layer.

The device performance of PLEDs has been improved by compensating for the drawbacks of PEDOT:PSS, nevertheless, fabrication of the PEDOT:PSS free PLEDs or the development of new hole transporting materials to replace PEDOT:PSS is strongly demanded in the aspect of device lifetime. Thermally and photo-cross-linkable polymers that possess hole transporting moiety have been extensively investigated in PLEDs because of their good solvent resistance for multilayer processing.[6,8,18–34] Triphenylamine and its derivatives such as *N*,*N*,*N*′,*N*′-tetraphenyl-1,1′-biphenyl-4,4′-diamine (TPD) and *N*,*N*′-bis(1-naphthyl)-*N*,*N*′-diphenyl-1,1′-biphenyl-4,4′-diamine (NPD) are well known hole transporting materials and constitute a key feature of many HTLs in OLEDs due to their high hole transporting and electron blocking/exciton blocking abilities that originate from their relatively high-lying HOMO (highest occupied molecular orbital) and large HOMO–LUMO gap (LUMO is the lowest unoccupied molecular orbital).[8,35]

Several groups have reported PLEDs with materials containing solution processable and thermally cross-linkable triphenylamine as alternatives to PEDOT:PSS for HTL.[20–24] Lim *et al.* reported PLED using thermally cross-linkable arylamine with trifluorovinyl ethers (TFVE) as HTL without PEDOT:PSS.[21] The cross-linked hole transporting polymeric layer was obtained by cyclopolymerization of the monomer at 230 °C for 2 h. The PLED with cross-linked HTL showed approximately one and half times higher device efficiency (cd A^{-1}) and two times higher luminance (cd m^{-2}) relative to PLED with PEDOT:PSS. Lim *et al.* synthesized an organosilicate polymer, based on *N*,*N*′-diphenyl-*N*,*N*′-bis(4-((*E*)-2-(triethoxysilyl)vinyl)phenyl)biphenyl-4,4′-diamine (TEVS–TPD), as a hole injection and transporting material using Heck and sol–gel chemistry.[24] The TEVS–TPD is fully cross-linked at 180 °C for 1 h. The performances of devices with TEVS–TPD as the HTL (6.4%, 12 900 cd m^{-2}) were comparable and/or superior to those based on PEDOT:PSS (6.4%, 8740 cd m^{-2}).

In this study, a novel thermally cross-linkable hole transporting polymer, which contains triphenylamine as a hole transporting moiety and ethynyl groups as the thermal cross-linker, was synthesized by living anionic polymerization and its possible use as an effective replacement of PEDOT:PSS was investigated by characterizing hole transporting, electron blocking abilities, and exciton quenching characteristics at the interface of EML. In general, well defined block copolymers, which have precise molecular structures that can influence film morphology and electronic device performance, can be designed and synthesized by living anionic polymerization.[36,37] Therefore, living anionic polymerization using a bidirectional initiator, potassium naphthalenide (K-Naph), was selected for the preparation of this hole transporting polymer in which ethynyl groups were positioned exactly at both ends of polymer chains. In addition, the thermal cross-linking of three ethynyl groups makes a benzene ring, which generates conjugation.[38–40] This may be beneficial for increasing the hole transporting abilities of the resulting block copolymer.

Experimental section

Materials

4,4′-Vinylphenyl-*N*,*N*-bis(4-*tert*-butylphenyl)benzenamine (**A**), trimethyl(2-(4-vinylphenyl)ethynyl)silane (**B**), and potassium naphthalenide (K-Naph) were prepared according to the literature.[41–43] These materials were diluted with tetrahydrofuran (THF) and divided into ampoules with break-seals on a vacuum line.

Measurements

^{1}H NMR spectra of the monomers and polymers were obtained using $CDCl_3$ as the solvent at 25 °C (JEOL JNM-ECX400). Chemical shifts were referred to tetramethylsilane (TMS) at 0 ppm. The FT-IR spectra were measured by a Perkins-Elmer Spectrum 2000 using KBr pellets. The polymers were characterized by size exclusion chromatography (SEC, Waters M77251, M510). The molecular weight of the homopolymer was measured by SEC with 4 columns (HR 0.5, HR 1, HR 3, and HR 4, Waters Styragel columns run in series; the pore sizes of the columns are 50, 100, 10^3, and 10^4 Å, respectively) with a refractive index detector at a flow rate of 1.0 mL min^{-1} using THF containing 2% triethylamine as the eluent at 40 °C and calibrated with polystyrene standards (American Polymer Standards Corp.). The thermal properties were investigated by thermogravimetric analysis (TA Instrument, TGA-Q50) and differential scanning calorimetry (TA Instrument, DSC-Q20) at a heating rate of 10 °C min^{-1} under nitrogen. UV-Vis absorption spectra were obtained using an Agilent 8453 UV-Vis spectrophotometer. Room temperature photoluminescence was measured by using some collection optics and a monochromator (Acton, SP-2150i) connected with a photomultiplier tube (Acton, PD-174). The second harmonic (SHG = 350 nm) of a tunable Ti:sapphire laser (Mira900, Coherent) with ~150 fs pulse width and 76 MHz repetition rate was used as the excitation source. The morphology of the cross-linked polymer film was investigated by atomic force microscopy (Nanoscope V, Veeco) in tapping mode. The electrochemical properties of the cross-linked film were measured by cyclic voltammetry (solartron analytical, SI 1280B) with a three-electrode cell consisting of a square of ITO glass as the working electrode, a platinum wire as the counter electrode, and Ag/AgCl as the reference electrode in a 0.10 M solution of tetrabutylammonium perchlorate in acetonitrile with a scan rate 50 mV s^{-1}.

Block copolymerization

The polymerization of **A** (0.821 mmol) was performed with K-Naph (0.0368 mmol) in THF at −78 °C for 0.5 h in an all glass apparatus equipped with break-seals under vacuum. After sampling for characterization of poly(**A**), **B** (0.307 mmol) was added to the living poly(**A**) solution and the reaction continued

at −78 °C for 0.5 h. The reaction solutions were poured into a large amount of methanol to obtain both poly(**A**) and poly(**B**-*b*-**A**-*b*-**B**) (P**BAB**). The yield of the block copolymer was quantitative. The resulting block copolymer was characterized by SEC, ^{1}H NMR, and FT-IR. P**BAB** (M_n(obsd) = 25 300, M_w/M_n = 1.11). ^{1}H NMR (400 MHz, $CDCl_3$): δ = 0.25 (SiCH_3), 1.05–2.25 (CH_2–CH and *tert*-butyl), 6.25–7.35 (triphenylamine and phenyl). FT-IR (KBr, cm^{-1}): 1250 (Si–CH_3), 2159 (C≡CSi$(CH_3)_3$).

Deprotection

P**BAB** (0.32 g) was stirred in 15 mL of dry THF. After tetra-*n*-butylammonium fluoride ($(C_4H_9)_4NF$) in THF (1.0 M, 10 mL) was added to the solution at 0 °C, the reaction mixture was stirred at 0 °C for 3 h. The reaction solution was poured into methanol to precipitate the polymer. The polymer was purified by reprecipitation in THF/methanol two times and freeze dried from a benzene solution under vacuum. The polymer yield was quantitative. The resulting deprotected polymer was characterized by SEC, ^{1}H NMR, and FT-IR. d-P**BAB** (M_n(obsd) = 24 300, M_w/M_n = 1.12). ^{1}H NMR (400 MHz, $CDCl_3$): δ = 1.05–2.25 (CH_2–CH and *tert*-butyl), 3.03 (C≡CH), 6.25–7.35 (triphenylamine and phenyl). FT-IR (KBr, cm^{-1}): 2109 (C≡C of C≡C–H), 3296 (C–H of C≡C–H).

Device fabrication

Glass substrate pre-coated with ITO was sequentially cleaned by ultrasonication with a detergent, deionized water, acetone and isopropyl alcohol. Surface treatment was performed by exposing the ITO to UV ozone. Solution of d-P**BAB** in toluene (0.8 wt%) was spin-coated at 5000 rpm for 20 s on ITO and then heated at 240 °C for 50 min under ambient conditions to complete the thermal cross-linking of the d-P**BAB** layer. The PEDOT:PSS (Al 4083) layer was also spin-coated on ITO and annealed at 150 °C for 10 min. The thicknesses of the cross-linked d-P**BAB** and PEDOT:PSS layers were 20 and 30 nm, respectively. After spin-coating the F8BT (35 nm, purchased from 1-material) on both the cross-linked d-P**BAB** and PEDOT:PSS layers, calcium (20 nm) and aluminum (80 nm) were sequentially deposited by thermal evaporation at a base pressure of 10^{-6} Torr. The multilayer PLEDs have structures of ITO/PEDOT:PSS (30 nm)/F8BT (35 nm)/Ca (20 nm)/Al (80 nm) and ITO/cross-linked d-P**BAB** (20 nm)/F8BT (35 nm)/Ca (20 nm)/Al (80 nm), respectively. The sample spot diameter is 4.64 mm^2. The device performances of the two PLEDs were investigated using a Keithley 2400 programmable source meter and a Spectroscan PR 650. The device fabrication and measurement were performed at room temperature in a glove box except for the spin-coating and annealing of PEDOT:PSS.

Time-correlated single photon counting (TCSPC)

TCPSC was performed to measure τ_{avr}. The second harmonic (SHG = 350 nm for d-P**BAB** excitation, 420 nm for F8BT excitation) of a tunable Ti:sapphire laser (Mira900, Coherent) with ~150 fs pulse width and 76 MHz repetition rate was used as the excitation source. The PL emission was spectrally resolved using some collection optics and a monochromator (Acton, SP-2150i). A TCSPC module (PicoQuant, PicoHarp) with a MCP-PMT (Hamamatsu, R3809U-59) was used for ultrafast detection. The total instrument response function (IRF) for the PL decay was less than 150 ps and the temporal time resolution was less than 10 ps. Deconvolution of the actual fluorescence decay and IRF was performed by using fitting software (FlouFit, PicoQuant) to deduce the time constant associated with each exponential decay.

Results and discussion

Block copolymerization

From a synthetic point of view, the successful living anionic polymerization of 4,4′-vinylphenyl-*N*,*N*-bis(4-*tert*-butylphenyl) benzenamine (**A**) can provide a well-defined block copolymer containing a poly(**A**) block by sequential block copolymerization.[41] Trimethyl(2-(4-vinylphenyl)ethynyl)silane (**B**) was chosen as the co-monomer for the preparation of a novel thermally cross-linkable polymer containing a triphenylamine moiety because the deprotection of the trimethylsilyl group from poly(**B**) offers an ethynyl group that can be used as a thermal cross-linker.[44] As shown in Scheme 1, poly(**B**-*b*-**A**-*b*-**B**) (P**BAB**) was synthesized through the sequential addition of **A** as the first monomer and **B** as the second monomer in the absence of any additives and the thermally cross-linkable polymer, d-poly(**B**-*b*-**A**-*b*-**B**) (d-P**BAB**), was subsequently prepared by a deprotection process.

As shown in Fig. 1a and b, the ^{1}H NMR spectra of the monomers and resulting block copolymer showed that polymerization proceeded exclusively. The signal of the vinyl group of the monomers disappeared, while the broad signal of the main polymer chain and the broad characteristic singlet of the *tert*-butyl group (1.20 ppm) and trimethylsilyl group (0.25 ppm) appeared. It was also shown by SEC measurements that the block copolymerization proceeded quantitatively. The polymerization results are summarized in Table 1. The resulting block copolymer had a predictable molecular weight (M_n) and narrow molecular weight distribution (M_w/M_n). The observed M_n value of P**BAB** was 25 300, which is close to the calculated value (M_n = 23 900). Furthermore, the SEC curve of P**BAB** was unimodal and narrow (M_w/M_n = 1.11) and completely shifted from the starting poly(**A**) toward the higher M_n region, as shown in Fig. 1d. These results suggest that the propagating chain-end derived from **A** can completely polymerize **B**, indicating that the polymerization of **B** was successfully conducted by living poly(**A**)

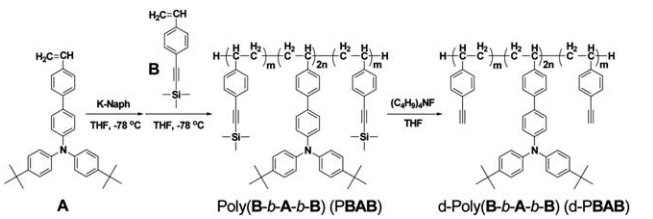

Scheme 1 Synthesis routes of poly(**B**-*b*-**A**-*b*-**B**) (P**BAB**) and d-poly(**B**-*b*-**A**-*b*-**B**) (d-P**BAB**) by living anionic polymerization and deprotection reaction.

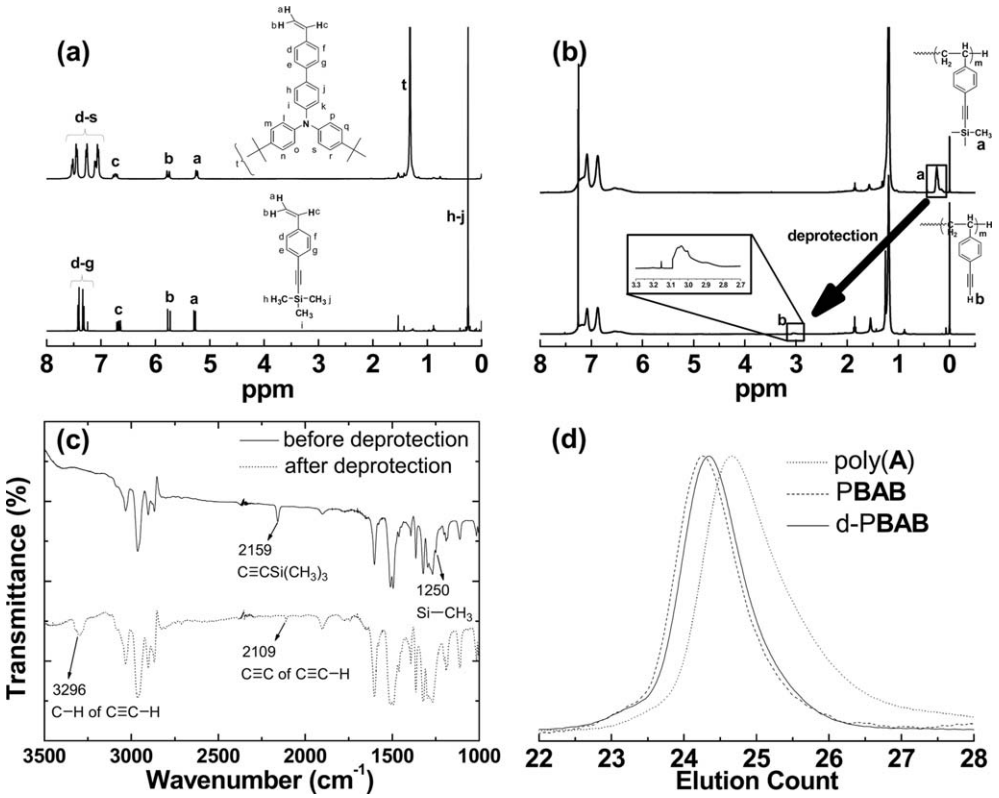

Fig. 1 ^{1}H NMR spectra of (a) monomers and (b) P**BAB** before and after deprotection. (c) FT-IR spectra of P**BAB** before and after deprotection. (d) SEC curves of poly(**A**), P**BAB**, and d-P**BAB**.

Table 1 Block copolymerization with K-Naph in THF at −78 °C[a]

Initiator mmol	Monomer 1st, mmol	Monomer 2nd, mmol	Block copolymer (homopolymer) $M_n \times 10^{-3}$ calcd[b]	obsd[c]	M_w/M_n[d]
0.0368	**A**, 0.821	**B**, 0.307	23.9 (20.5)	25.3 (22.0)	1.11 (1.09)

[a] Polymer yield was quantitative. Polymerization time was total 1 h, 0.5 h for **A** and 0.5 h for **B**. [b] M_n (calcd) = (molecular weight of monomer) × [monomer] × 2/[initiator]. [c] M_n of the block copolymer was determined by using M_n of the homopolymer and the molar ratio of each block estimated by ^{1}H NMR. [d] M_w/M_n was obtained by SEC calibration using polystyrene standards in THF solution containing 2% triethylamine as the eluent at 40 °C.

without any side reactions under these polymerization conditions.

Deprotection

The deprotection of the trimethylsilyl group from P**BAB** was carried out to prepare the well-defined block copolymer with thermally cross-linkable ethynyl groups. The success of the deprotection was confirmed by ^{1}H NMR, FT-IR and SEC. In the ^{1}H NMR spectra shown in Fig. 1b, it was found that the signal of the methyl proton of the trimethylsilyl group at 0.25 ppm disappeared and the signal of the ethynyl proton newly appeared at 3.03 ppm. FT-IR spectra also exhibited complete conversion of the (trimethylsilyl)ethynyl group to the ethynyl group. Fig. 1c showed that the new bands were observed at 2109 (C≡C of C≡C–H) and 3296 cm^{-1} (C–H of C≡C–H), respectively, while the characteristic bands of the Si–CH_3 and C≡C$Si(CH_3)_3$ at 1250 and 2159 cm^{-1} disappeared. Additional evidence for the deprotection was given by SEC. The SEC curve of the deprotected polymer was still unimodal and clearly shifted from the elution volume of P**BAB** toward the lower M_n region, as shown in Fig. 1d. It was also observed that the M_w/M_n of d-P**BAB** was almost same as that of P**BAB**, meaning that no side reactions occurred during the course of the deprotection. Accordingly, it can be indicated from these analytical results that the deprotection process was successfully performed to give a thermally cross-linkable block copolymer containing triphenylamine moieties.

Characterization of deprotected block copolymer

The thermal stability of d-P**BAB** (5 wt% loss at 392 °C) was investigated by thermogravimetric analysis (TGA) under nitrogen (Fig. S1 in the ESI†). As shown in Fig. 2a, the glass transition temperature (T_g) and a large exothermic peak were observed at ~199 and ~240 °C, respectively, on the 1st scan of the DSC thermogram of d-P**BAB**. However, during the 2nd scan, an intense exothermic peak was not observed until approximately 300 °C and the T_g was estimated to be ~225 °C, which is higher than that determined from the 1st scan due to a thermal cross-linking reaction between the ethynyl groups. The DSC

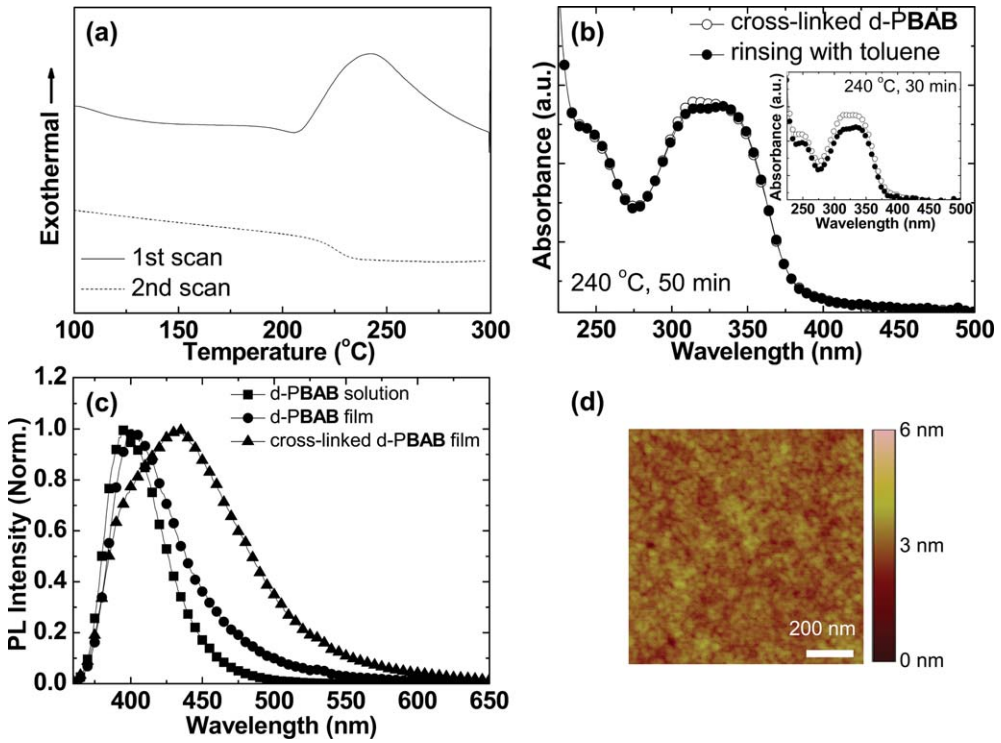

Fig. 2 (a) Differential scanning calorimetry (DSC) thermogram of d-P**BAB** under nitrogen with a heating rate of 10 °C min^{-1}. (b) UV-Vis absorption spectra of d-P**BAB** film cross-linked at 240 °C for 50 min before and after being washed with toluene (inset: UV-Vis absorption spectra of d-P**BAB** film cross-linked at 240 °C for 30 min before and after being washed with toluene). (c) Photoluminescence (PL) spectra of d-P**BAB** solution, d-P**BAB** film before and after thermal cross-linking at 240 °C for 50 min. (d) Atomic force microscopy (AFM) image of d-P**BAB** film cross-linked at 240 °C for 50 min.

results reflects that the ethynyl groups in d-P**BAB** were cross-linked during heating.[45,46]

The solvent resistance of cross-linked d-P**BAB** was investigated by spin-coating a good solvent for d-P**BAB**. As shown in the inset of Fig. 2b, the absorption spectrum of d-P**BAB** cross-linked at 240 °C for 30 min changed after rinsing with toluene, however, no absorption spectral change was observed when d-P**BAB** was heated at the same temperature for a longer time (50 min). This unchanged absorption spectrum indicates that a high solvent resistance for the cross-linked d-P**BAB** film was achieved by thermal treatment at 240 °C for 50 min.

Fig. 2c shows the PL spectra of the d-P**BAB** solution, d-P**BAB** film and cross-linked d-P**BAB** film. The PL spectrum of the d-P**BAB** film became somewhat broadened and red-shifted relative to the d-P**BAB** solution. Interestingly, the PL spectrum of the cross-linked d-P**BAB** film differed significantly from that of the d-P**BAB** film. The major PL peak of cross-linked d-P**BAB** film (433 nm) was red-shifted by approximately 30 nm from that of the d-P**BAB** film and the PL spectrum of cross-linked film had a full width at half maximum (FWHM) that broadened from 42 to 100 nm after cross-linking. This result suggests that the thermal cross-linking reaction resulted in an increase of film density and closer packing of the chromophores.[47] These behaviours might facilitate and/or enhance the hole transporting process through hopping between chromophores as a result of the enhanced π-electron overlap.[19] Moreover, the poor PL intensity of the cross-linked d-P**BAB** film might prevent excimer and/or exciplex formation, enhancing the color purity of device. The PL lifetime of the d-P**BAB** solution, d-P**BAB** film, and cross-linked d-P**BAB** film are summarized in Fig. S2 and Table S1 in the ESI.† The τ_{avr} of the d-P**BAB** solution at 430 nm was 1.10 ns, while τ_{avr} of the d-P**BAB** film (0.55 ns) and cross-linked d-P**BAB** film (0.35 ns) drastically decreased. The significant decrease in τ_{avr} of the cross-linked d-P**BAB** film resulting from an increase of film density and closer packing of the chromophores led to the poor PL intensity of the cross-linked d-P**BAB** film.

The surface morphology of the HTLs is also a critical factor for efficient PLEDs. The surface morphology of cross-linked d-P**BAB** film was studied by AFM, as shown in Fig. 2d. After cross-linking, the root mean square (RMS) roughness of the d-P**BAB** film was 0.2 nm, which is sufficiently smooth for the effective planarization of the ITO surface whose RMS roughness was determined to be 3.0–3.7 nm by AFM.[27]

The HOMO and LUMO energy levels of the cross-linked d-P**BAB** were calculated by cyclic voltammetry (CV) and using the optical band gap (Fig. S3 in the ESI†).[21,27,47] As shown in Fig. 3a, the LUMO energy level of the cross-linked d-P**BAB** is −1.85 eV, which is higher than that of PEDOT:PSS (−3.40 eV). Such a high-lying LUMO level of cross-linked d-P**BAB** makes it an efficient electron blocking layer for the emissive polymer, poly(9,9′-dinoctylfluorene-*alt*-benzothiadiazole) (F8BT), and thus results in improved efficiency for the PLED. Commercially available F8BT, a polyfluorene derivative, was used as the emissive polymer due to its remarkable opto-electronic properties such as good processability, air and thermal stability, high PL efficiency, and high electron mobility.[48–51] Furthermore, it is expected that

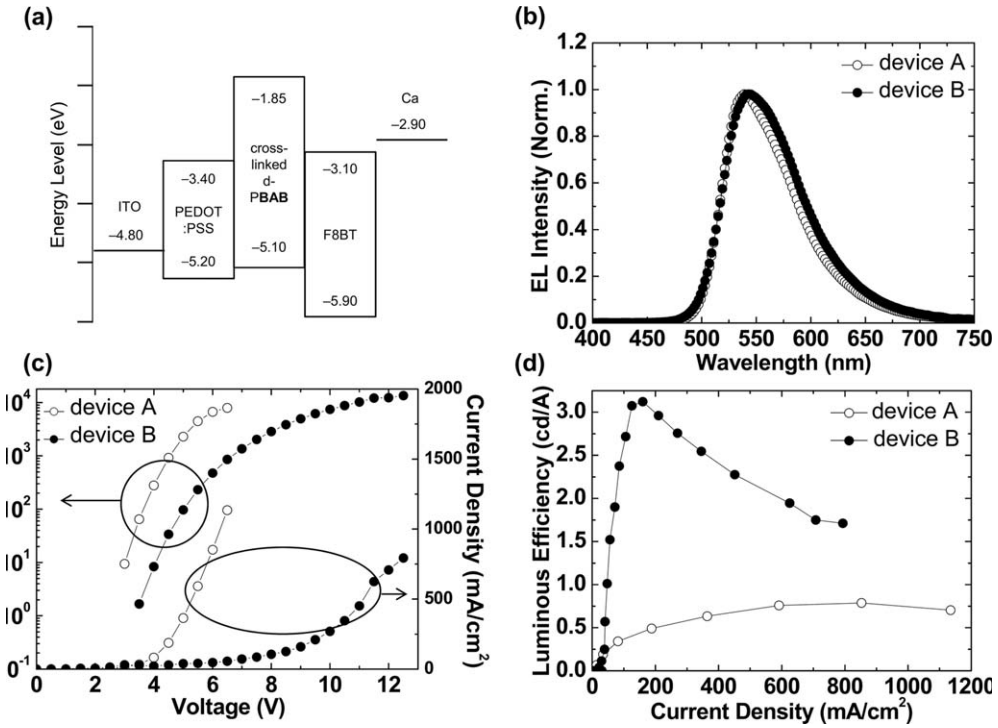

Fig. 3 (a) Energy level diagrams. (b) Electroluminescence (EL) spectra, (c) current density and luminance *versus* voltage and (d) luminous efficiency *versus* current density characteristics of device A (ITO/PEDOT:PSS/F8BT/Ca/Al) and B (ITO/cross-linked d-P**BAB**/F8BT/Ca/Al).

the HOMO energy level of the cross-linked d-P**BAB** (−5.10 eV), located between that of ITO (−4.80 eV) and F8BT (−5.90 eV), can facilitate hole transport. From the results of various characterizations, it was apparent that the high solvent resistance, defect free surface, hole transporting properties, and excellent electron blocking properties allowed the cross-linked d-P**BAB** film to be a promising HTL for solution processed multilayer PLEDs with high efficiency.

PLED device performance

Multilayer PLEDs with the device structures of ITO/PEDOT:PSS/F8BT/Ca/Al and ITO/cross-linked d-P**BAB**/F8BT/Ca/Al were fabricated to evaluate the hole transporting, electron and exciton blocking abilities of cross-linked d-P**BAB**. The device with PEDOT:PSS as the HIL and HTL was prepared for reference. The PEDOT:PSS based and cross-linked d-P**BAB** based PLEDs hereafter are simply designated as devices A and B, respectively.

As shown in Fig. 3b, the electroluminescence (EL) spectra of both devices A and B were almost the same and no emission from the cross-linked d-P**BAB** was observed. This indicates that the recombination of holes and electrons occurred in the EML. Fig. 3c and d show the current density and luminance *versus* voltage and luminous efficiency *versus* current density characteristics of devices A and B. Device B showed a maximum luminance (L_{max}) of 13 600 cd cm^{-2} and a maximum luminous efficiency of 3.2 cd A^{-1}, which are approximately one and a half and four times higher than those of device A (8000 cd cm^{-2}, 0.78 cd A^{-1}), respectively. Device B also showed a lower current density (790 mA cm^{-2}) and a slightly higher turn-on voltage (3.5 V) than those of device A (1130 mA cm^{-2}, 3.0 V). The device performance of device A such as current density and luminous efficiency is similar to the reported value.[5] Therefore, the PLED based on polyfluorene derivative is qualified to evaluate the difference in device performance based on the different hole transporting materials.

The improved performance of device B can be explained by two primary reasons. First, the excellent electron and exciton blocking abilities of the cross-linked d-P**BAB** attributed to the higher LUMO level lead to a balanced charge recombination in the emissive layer. The outstanding electron blocking characteristics of the cross-linked d-P**BAB** was verified by the lower current density of device B. In contrast, in the device A, considerable electrons pass through the F8BT without recombination with holes and are drained at the ITO anode through the highly conductive PEDOT:PSS layer due to its weak electron blocking abilities, leading to a lower electron and hole recombination efficiency and hence a lower overall device efficiency. The cross-linked d-P**BAB** also showed effective electron blocking abilities to MEH-PPV (LUMO: −2.80 eV). Second, less exciton quenching at the interface between the cross-linked d-P**BAB** and F8BT increases the radiative decay of the F8BT. The degree of exciton quenching of F8BT will be explained in the time-correlated single photon counting (TCSPC) results and discussion section. A slightly higher turn-on voltage for device B might be due to the relatively lower hole mobility of the cross-linked d-P**BAB** than PEDOT:PSS (10^{-2} to 10^{-3} cm^2 (V^{-1} s))[52] originated from the non-conjugated vinyl group.[22,24] The lower turn-on voltage of device B might be attained by blending a strong

electron acceptor such as 1,1,2,2-tetrafluorotetracyanoquinodimethane (F4-TCNQ),[53,54] fullerene (C_{60}),[55,56] and [6,6]-phenyl C_{61} butyric acid methyl ester (PCBM)[57] and thus further studies are currently under investigation.

TCSPC characterization

To prove the abilities of the cross-linked d-P**BAB** for the prevention and/or reduction of exciton quenching, the exciton lifetime (τ_{avr}) of F8BT with different HTLs was measured using time-correlated single photon counting (TCSPC). For TCSPC measurements, F8BT with thicknesses of 10, 35, and 65 nm were spin-coated on PEDOT:PSS and the cross-linked d-P**BAB** under the same conditions as device fabrication. A sample with a configuration of quartz/F8BT was prepared for reference. Fig. 4b shows the PL decay profile of F8BT with a thickness of 35 nm, which is same film thickness of the F8BT in device. The τ_{avr} of F8BT at 545 nm dramatically decreased from 1.82 ns on quartz to 1.37 ns on PEDOT:PSS. However, no significant decrease in τ_{avr} was found when cross-linked d-P**BAB** was used as the HTL. The τ_{avr} of F8BT on cross-linked d-P**BAB** at 545 nm was 1.69 ns, which is approximately 93% of the τ_{avr} of F8BT on quartz. This result demonstrates that exciton quenching of F8BT at the interface of cross-linked d-P**BAB** is much less than that at the interface of PEDOT:PSS, as shown in Fig. 4b and Table 2.

The changes in τ_{avr} of F8BT with different thickness were also investigated (Fig. 4 and Table 2). The τ_{avr} of F8BT on PEDOT:PSS was considerably influenced by the film thickness of F8BT, as shown in Fig. 4d. At the interface of PEDOT:PSS, less exciton quenching of F8BT was found in the thicker film

Table 2 Exciton lifetimes (τ_{avr}) of F8BT on different HTLs[a]

Samples	$\tau_1(f_1)$, ns	$\tau_2(f_2)$, ns	χ^2	τ_{avr}, ns
Quartz/F8BT[b]	1.71	—	1.78	1.71
Cross-linked d-P**BAB**/F8BT[b]	1.85 (0.61)	0.90 (0.39)	1.50	1.48
PEDOT:PSS/F8BT[b]	1.05 (0.76)	0.42 (0.24)	1.19	0.90
Quartz/F8BT[c]	1.82	—	1.75	1.82
Cross-linked d-P**BAB**/F8BT[c]	1.82 (0.86)	0.83 (0.14)	1.62	1.69
PEDOT:PSS/F8BT[c]	1.50 (0.85)	0.60 (0.15)	1.54	1.37
Quartz/F8BT[d]	1.77	—	1.67	1.77
Cross-linked d-P**BAB**/F8BT[d]	1.80 (0.92)	0.65 (0.08)	1.62	1.70
PEDOT:PSS/F8BT[d]	1.55 (0.87)	0.57 (0.13)	1.50	1.42

[a] Monitored wavelength was 545 nm. The PL decay curves were fitted with either a monoexponential or a biexponential function to calculate the lifetime of F8BT. The PL decay curves of quartz/F8BT films were fitted with a monoexponential function and those of the PEDOT:PSS/F8BT and cross-linked d-P**BAB**/F8BT films were fitted with a biexponential function. The amplitude weighted average exciton lifetime (τ_{avr}) was $f_1\tau_1 + f_2\tau_2$, where f_1 and f_2 are fractional intensities and τ_1 and τ_2 are lifetimes. [b] The thickness of F8BT is 10 nm. [c] The thickness of F8BT is 35 nm. [d] The thickness of F8BT is 65 nm.

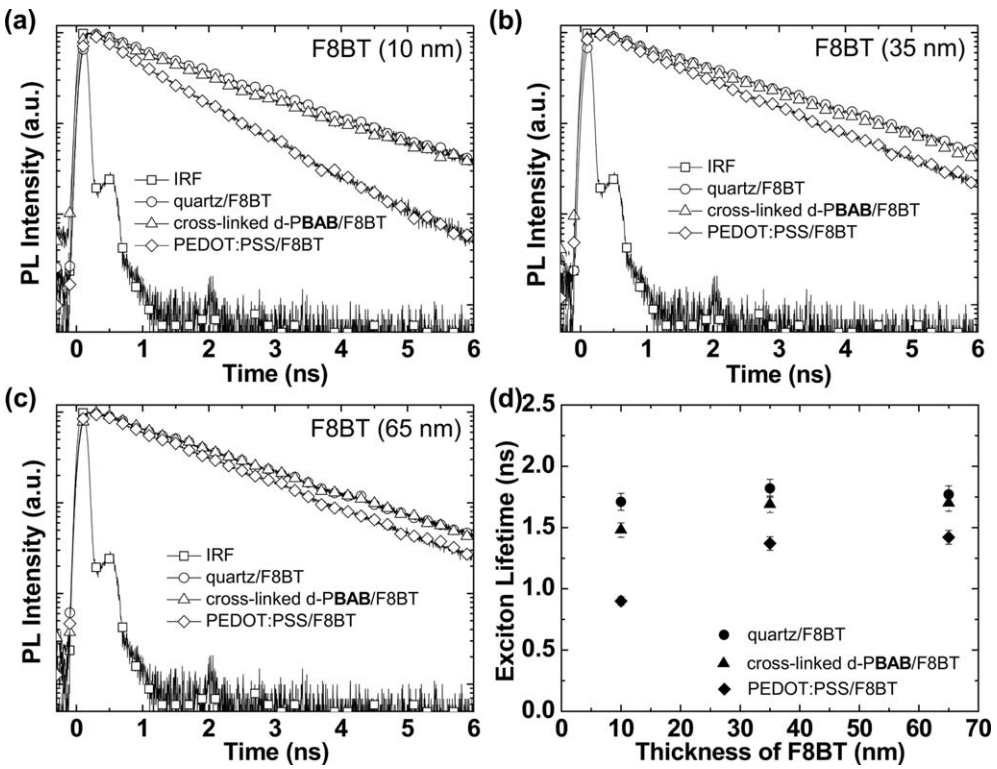

Fig. 4 PL decay profiles of F8BT with a thickness of (a) 10 nm, (b) 35 nm, and (c) 65 nm. (d) Exciton lifetime (τ_{avr}) of F8BT as a function of F8BT film thickness on different HTLs. The F8BT was excited at 420 nm and the monitored wavelength was 545 nm. The PL decay curves were fitted with either a monoexponential or a biexponential function to calculate the lifetime of F8BT. The PL decay curves of quartz/F8BT films were fitted with a monoexponential function and those of PEDOT:PSS/F8BT and cross-linked d-P**BAB**/F8BT films were fitted with a biexponential function. The amplitude weighted average exciton lifetime (τ_{avr}) was $f_1\tau_1 + f_2\tau_2$, where f_1 and f_2 are fractional intensities and τ_1 and τ_2 are lifetimes.

(65 nm) than in the thinner film (10 nm). The reduction of τ_{avr} was 47% (20%) in 10 nm (65 nm) F8BT films. This result suggests that the exciton diffusion length of F8BT is ~10 nm, which is similar to that observed for other conjugated polymers.[58–62] The less exciton quenching of F8BT in thicker film might be explained by the reduction of any chemical and physical quenching due to the increased distance of the F8BT excitons from the PEDOT:PSS quenching interface. However, the exciton quenching of F8BT was significantly reduced even with 10 nm thick F8BT when PEDOT:PSS was replaced by cross-linked d-P**BAB**. The reduction of τ_{avr} was only 13% (4%) in 10 nm (65 nm) film. These results suggest excellent abilities of the cross-linked d-P**BAB** to prevent and/or reduce exciton quenching, leads to a strong reduction in the non-radiative decay rate, which results in improved device performance.

Conclusions

A novel thermally cross-linkable polymer (d-P**BAB**) possessing triphenylamine as a hole transporting moiety and ethynyl groups as a thermal cross-linker was synthesized by the combination of living anionic polymerization and a deprotection process. The d-P**BAB** showed excellent solvent resistance, defect free surfaces, hole transporting and excellent electron blocking properties. PLED with cross-linked d-P**BAB** as the HTL exhibited approximately one and half and four times higher luminance and luminous efficiency than those of device with PEDOT:PSS. These results are ascribed to the excellent abilities of the cross-linked d-P**BAB** to block electrons and excitons as well as to prevent and/or reduce exciton quenching, suggesting that the d-P**BAB** synthesized in this work is a promising material for the replacement of conventional PEDOT:PSS for realizing highly efficient PLEDs. It is also expected that PLED with cross-linked d-P**BAB** will show longer device lifetime than that of device with PEDOT:PSS due to the no acidity of cross-linked d-P**BAB**.

Acknowledgements

This work was supported by the Program for Integrated Molecular System (PIMS) at Gwangju Institute of Science and Technology, the World-Class University Program funded by the Ministry of Education, Science and Technology (MEST) through the National Research Foundation of Korea (R31-10026), the Basic Science Research Program (Project no. 2011-0026341) and the Happy Tech Program (Project no. 2011-0020956) funded by the Ministry of Education, Science and Technology (MEST) through the National Research Foundation of Korea, and APRI-Research Program through a grant provided by Gwangju Institute of Science and Technology.

References

1 J. H. Burroughes, D. D. C. Bradley, A. R. Brown, R. N. Marks, K. Mackay, R. H. Friend, P. L. Burns and A. B. Holmes, *Nature*, 1990, **347**, 539.
2 A. Kraft, A. C. Grimsdale and A. B. Holmes, *Angew. Chem., Int. Ed.*, 1998, **37**, 403.
3 X. Gong, S. Wang, D. Moses, G. C. Bazan and A. J. Heeger, *Adv. Mater.*, 2005, **17**, 2053.
4 Y. Sun, N. C. Giebink, H. Kanno, B. Ma, M. E. Thompson and S. R. Forrest, *Nature*, 2006, **440**, 908.
5 H. Yan, B. J. Scott, Q. Huang and T. J. Marks, *Adv. Mater.*, 2004, **16**, 1948.
6 Y.-H. Niu, M. S. Liu, J.-W. Ka, J. Bardeker, M. T. Zin, R. Schofield, Y. Chi and A. K.-Y. Jen, *Adv. Mater.*, 2007, **19**, 300.
7 J.-S. Kim, R. H. Friend, I. Grizzi and J. H. Burroughes, *Appl. Phys. Lett.*, 2005, **87**, 023506.
8 H. Yan, P. Lee, N. R. Armstrong, A. Graham, G. A. Evmenenko, P. Dutta and T. J. Marks, *J. Am. Chem. Soc.*, 2005, **127**, 3172.
9 J. E. Yoo, K. S. Lee, A. Garcia, J. Tarver, E. D. Gomez, K. Baldwin, Y. Sun, H. Meng, T.-Q. Nguyen and Y.-L. Loo, *Proc. Natl. Acad. Sci. U. S. A.*, 2010, **107**, 5712.
10 M.-R. Choi, S.-H. Woo, T.-H. Han, K.-G. Lim, S.-Y. Min, W. M. Yun, O. K. Kwon, C. E. Park, K.-D. Kim, H.-K. Shin, M.-S. Kim, T. Noh, J. H. Park, K.-H. Shin, J. Jang and T.-W. Lee, *ChemSusChem*, 2011, **4**, 363.
11 A. V. Dijken, A. Perro, E. A. Meulenkamp and K. Brunner, *Org. Electron.*, 2003, **4**, 131.
12 J.-S. Kim, P. K. H. Ho, C. E. Murphy, A. J. A. B. Seeley, I. Grizzi, J. H. Burroughes and R. H. Friend, *Chem. Phys. Lett.*, 2004, **386**, 2.
13 T. P. Nguyen and S. A. de Vos, *Appl. Surf. Sci.*, 2004, **221**, 330.
14 J. Y. Lee, *Synth. Met.*, 2006, **156**, 537.
15 M. P. de Jong, L. J. van Ijzendoorn and M. J. A. de Voigt, *Appl. Phys. Lett.*, 2000, **77**, 2255.
16 K. W. Wong, H. L. Yip, Y. Luo, K. Y. Wong, W. M. Lau, K. H. Low, H. F. Chow, Z. Q. Gao, W. L. Yeung and C. C. Chang, *Appl. Phys. Lett.*, 2002, **80**, 2788.
17 J. Morgado, R. H. Friend and F. Cacialli, *Appl. Phys. Lett.*, 2002, **80**, 2436.
18 S. Liu, X. Jiang, H. Ma, M. S. Liu and A. K.-Y. Jen, *Macromolecules*, 2000, **33**, 3514.
19 X. Jiang, S. Liu, M. S. Liu, P. Herguth, A. K.-Y. Jen, H. Fong and M. Sarikaya, *Adv. Funct. Mater.*, 2002, **12**, 745.
20 H. Yan, Q. Huang, B. J. Scott and T. J. Marks, *Appl. Phys. Lett.*, 2004, **84**, 3873.
21 B. Lim, J.-T. Hwang, J. Y. Kim, J. Ghim, D. Vak, Y.-Y. Noh, S.-H. Lee, K. Lee, A. J. Heeger and D.-Y. Kim, *Org. Lett.*, 2006, **8**, 4703.
22 G. K. Paul, J. Mwaura, A. A. Argun, P. Taranekar and J. R. Reynolds, *Macromolecules*, 2006, **39**, 7789.
23 M. S. Liu, Y.-H. Niu, J.-W. Ka, H.-L. Yip, F. Huang, J. Luo, T.-D. Kim and A. K.-Y. Jen, *Macromolecules*, 2008, **41**, 9570.
24 Y. Lim, Y.-S. Park, Y. Kang, D. Y. Jang, J. H. Kim, J.-J. Kim, A. Sellinger and D. Y. Yoon, *J. Am. Chem. Soc.*, 2011, **133**, 1375.
25 Y.-H. Niu, M. S. Liu, J.-W. Ka and A. K.-Y. Jen, *Appl. Phys. Lett.*, 2006, **88**, 093505.
26 B. Ma, F. Lauterwasser, L. Deng, C. S. Zonte, B. J. Kim, J. M. J. Fréchet, C. Borek and M. E. Thompson, *Chem. Mater.*, 2007, **19**, 4827.

27 Y.-J. Cheng, M. S. Liu, Y. Zhang, Y. Niu, F. Huang, J.-W. Ka, H.-L. Yip, Y. Tian and A. K.-Y. Jen, *Chem. Mater.*, 2008, **20**, 413.
28 D. F. O'Brien, P. E. Burrows, S. R. Forrest, B. E. Koene, D. E. Loy and M. E. Thompson, *Adv. Mater.*, 1998, **10**, 1108.
29 F. Huang, Y. J. Cheng, Y. Zhang, M. S. Liu and A. K.-Y. Jen, *J. Mater. Chem.*, 2008, **18**, 4495.
30 C. A. Zuniga, S. Barlow and S. R. Marder, *Chem. Mater.*, 2011, **23**, 658.
31 Y.-D. Zhang, R. D. Hreha, G. E. Jabbour, B. Kippelen, N. Peyghambarian and S. R. Marder, *J. Mater. Chem.*, 2002, **12**, 1703.
32 E. Bacher, M. Bayerl, P. Rudati, N. Reckefuss, C. D. Müller, K. Meerholz and O. Nuyken, *Macromolecules*, 2005, **38**, 1640.
33 S. Jungermann, N. Riegel, D. Müller, K. Meerholz and O. Nuyken, *Macromolecules*, 2006, **39**, 8911.
34 J. Schelter, G. F. Mielke, A. Köhnen, J. Wies, S. Köber, O. Nuyken and K. Meerholz, *Macromol. Rapid Commun.*, 2010, **31**, 1560.
35 Y. Shirota, *J. Mater. Chem.*, 2000, **10**, 1.
36 B. Ma, B. J. Kim, L. Deng, D. A. Poulsen, M. E. Thompson and J. M. J. Fréchet, *Macromolecules*, 2007, **40**, 8156.
37 N.-G. Kang, B. Cho, B.-G. Kang, S. Song, T. Lee and J.-S. Lee, *Adv. Mater.*, 2012, **24**, 385.
38 S. Saito and Y. Yamamoto, *Chem. Rev.*, 2000, **100**, 2901.
39 K.-S. Lee, M.-H. Jeong, J.-P. Lee and J.-S. Lee, *Macromolecules*, 2009, **42**, 584.
40 A. Qin, C. K. W. Jim, W. Lu, J. W. Y. Lam, M. Häussler, Y. Dong, H. H. Y. Sung, I. D. Williams, G. K. L. Wong and B. Z. Tang, *Macromolecules*, 2007, **40**, 2308.
41 B.-G. Kang, N.-G. Kang and J.-S. Lee, *Macromolecules*, 2010, **43**, 8400.
42 T. Ishizone, A. Hirao, S. Nakahama, T. Kakuchi, K. Yokota and K. Tsuda, *Macromolecules*, 1991, **24**, 5230.
43 K. Tsuda, T. Ishizone, A. Hirao, S. Nakahama, T. Kakuchi and K. Yokota, *Macromolecules*, 1993, **26**, 6985.
44 K. Tsuda, W. Hirahata, K. Yokota, T. Kakuchi, T. Ishizone and A. Hirao, *Polym. Bull.*, 1997, **39**, 173.
45 J.-P. Kim, W.-Y. Lee, J.-W. Kang, S.-K. Kwon, J.-J. Kim and J.-S. Lee, *Macromolecules*, 2001, **34**, 7817.
46 K.-S. Lee and J.-S. Lee, *Chem. Mater.*, 2006, **18**, 4519.
47 W.-F. Su, R.-T. Chen and Y. Chen, *J. Polym. Sci., Part A: Polym. Chem.*, 2011, **49**, 352.
48 D. Neher, *Macromol. Rapid Commun.*, 2001, **22**, 1365.
49 U. Scherf and E. J. W. List, *Adv. Mater.*, 2002, **14**, 477.
50 A. J. Campbell, D. D. C. Bradley and H. Antoniadis, *Appl. Phys. Lett.*, 2001, **79**, 2133.
51 Y. Kim, S. Cook, S. A. Choulis, J. Nelson, F. R. Durrant and D. D. C. Bradley, *Chem. Mater.*, 2004, **16**, 4812.
52 D. A. Bernards and G. G. Malliaras, *Adv. Funct. Mater.*, 2007, **17**, 3538.
53 X. Zhou, J. Blochwitz, M. Pfeiffer, A. Nollau, T. Fritz and K. Leo, *Adv. Funct. Mater.*, 2001, **11**, 310.
54 K. S. Yook and J. Y. Lee, *Electrochem. Solid-State Lett.*, 2012, **15**, J11.
55 J. Y. Lee and J. H. Kwon, *Appl. Phys. Lett.*, 2005, **86**, 063514.
56 J. Y. Lee and J. H. Kwon, *Appl. Phys. Lett.*, 2006, **88**, 183502.
57 G. Yan, S. Zhao, Z. Xu, F. Zhang, C. Kong, X. Liu, W. Gong and X. Xu, *Phys. Status Solidi A*, 2011, **208**, 2317.
58 J. J. M. Halls, K. Pichler, R. H. Friend, S. C. Moratti and A. B. Holmes, *Appl. Phys. Lett.*, 1996, **68**, 3120.
59 A. Haugeneder, M. Neges, C. Kallinger, W. Spirkl, U. Lemmer, J. Feldmann, U. Scherf, E. Harth, A. Gügel and K. Müllen, *Phys. Rev. B: Condens. Matter Mater. Phys.*, 1999, **59**, 15346.
60 T. Stübinger and W. Brütting, *J. Appl. Phys.*, 2001, **90**, 3632.
61 D. E. Markov, E. Amsterdam, P. W. M. Blom, A. B. Sieval and J. C. Hummelen, *J. Phys. Chem. A*, 2005, **109**, 5266.
62 D. E. Markov, C. Tanase, P. W. M. Blom and J. Wildeman, *Phys. Rev. B: Condens. Matter Mater. Phys.*, 2005, **72**, 045217.